Scientia Iranica, Vol. 10, No. 2, pp 175–185

SCIENTIA
IRANICA

A New Method for Predicting the Amplitude and Frequency of a Highly Swept Wing Undergoing Rocking Motion

M.R. Soltani*, A. Ebrahimi[1] and A.R. Davari[1]

Wing rock motion can be described as an oscillatory bank angle buildup to a constant amplitude rocking motion. This phenomenon is realized for delta wings with more than 74 degrees leading edge sweep angles, where asymmetric vortex shedding occurs before vortex breakdown. For wings with sweep angles less than 74 degrees, rocking motion occurs if the wing is in a yawed situation. In this paper, a new and simple method has been presented to predict the amplitude and frequency of oscillation of delta wings undergoing rocking motion at high angles of attack. The predicted data are in excellent agreement with those obtained by experimental studies for wings with sweep angles of 76 and 80 degrees.

INTRODUCTION

The steadily increasing demands on performance expose present day aerospace vehicles to unsteady flow fields that generate highly nonlinear aerodynamics. This phenomenon exhibits significant coupling between longitudinal and lateral degrees of freedom.

To maintain air superiority, present and future aircraft will be expected to perform complex controlled maneuvers at high angles of attack, exceeding their maximum static lift (post-stall condition). The need to achieve an advantageous first firing opportunity and, perhaps, to transit rapidly to a second target, adds another element of dynamic maneuvering to future combat aircraft. Post-stall maneuvering is performed at relatively low forward speed, i.e. subsonic, where the vehicle trades kinetic energy for potential energy.

The transition between targets requires high-speed maneuverability. Therefore, the design of advanced fighters for both air-to-surface and air-to-air tactical roles presents a challenge, due to the wide spectrum of operational requirements. Since different configurations have advantages and disadvantages with respect to different problem areas, future fighter aircraft should possess the following performance attributes [1]:

- Efficient cruise capability at subsonic and supersonic flight;
- Rapid acceleration and deceleration;
- Post-stall pitch pointing capability;
- Supermaneuverability, i.e. low speed, high turn rate and low turning radius;
- Lateral agility.

It is desirable, not only to incorporate the above qualities in future aircraft design but, also, to find a low-cost way of improving the maneuvering effectiveness of current fighters, while retaining the existing engines. The aerodynamic requirements for each condition often present conflicting demands. For example, the need to rapidly accelerate from subsonic to supersonic cruise conditions requires highly swept, low aspect ratio thin wings. However, low level high-speed penetration missions require high wing loading with moderate sweep, i.e. conventional trapezoidal wings. These conflicts in the design of tactical fighters pose significant engineering and technological challenges; thus, a compromise should be made between optimum supersonic cruise and low speed maneuvering.

For supermaneuverable aircraft, flight at a high angle of attack is an inherent part of both offensive and defensive maneuvering. Typical modern fighter aircraft achieve maximum lift at an angle of attack in

*. *Corresponding Author, Department of Aerospace Engineering, Sharif University of Technology, P.O. Box 11365-9567, Tehran, I.R. Iran.*

1. *Department of Aerospace Engineering, Sharif University of Technology, P.O. Box 11365-9567, Tehran, I.R. Iran.*

the range of 25-35 degrees. Since conventional wings achieve their maximum lift at incidence well below the desired value, advanced delta wing configurations lend themselves particularly well to the application of post stall maneuverability without deterioration in their required supersonic performance. In fact, many of the present day advanced tactical fighters utilize highly swept wings with relatively sharp leading edges. Others use low sweep trapezoidal wing platforms but combine these with highly swept strakes for advanced maneuverability at high angles of attack (i.e. F-16 and F-18). However, the most typical wing, representing the type of flow common to all, is the delta wing.

The flow structure over a delta wing at moderate to high angles of attack is different than that of conventional low sweep wings. For sharp leading edge delta wings at a zero angle of attack, the flow remains attached over both surfaces and no lift is generated. As soon as the angle of attack departs from zero, their sharp leading edge prevents the approaching flow from remaining attached to the surface. The separated shear layer rolls up into two primary vortices, which start at the apex of the wing and proceed downstream in the direction of the flow (see Figures 1 and 2).

The onset of the leading edge vortices is distinguished by the character of the aerodynamic coefficients, namely, by the pronounced nonlinearity of the forces and moments with respect to the angle of attack. The size and strength of these vortices increase with an increasing angle of attack and become a dominant feature of the flow at moderate to high angles of attack. Depending on the wing sweep angle, these vortices remain stable through a wide range of angles of attack (up to an angle of 40 degrees for an 85 degree sweep angle with an aspect ratio of 0.35) and the flow is characteristically steady. Hence, they have an important effect on the aerodynamic forces and moments of delta wings.

Delta wing vortices contain a great deal of energy which increases rapidly with the angle of attack. This energy induces additional velocity on the upper surface of the wing, reducing the pressure considerably. In consequence, an additional lift force, known as vortex lift, is generated, which increases non-linearly with increasing angle of attack. This lift, which accounts for about 50 percent of the total lift, can be used to improve landing capability [1].

Vortex lift is also a leading contributor in gaining the tactical advantage desired in a combat environment. The generation of vortex-induced lift results in an extension of the maneuvering capability of the fighter aircraft, which, in turn, requires that both longitudinal and lateral directional stability and control be maintained in this extended angle of attack range. The highly swept leading edge of the delta wing also provides favorable drag characteristics at high speed, making supersonic flight practical.

However, a limit to the favorable effect induced by leading edge vortices is reached once the angle of attack attains values where a sudden and dramatic structural change in the vortices, known as vortex breakdown, occurs (Figure 3). Vortex bursting is associated with an abrupt axial flow deceleration, expansion of the vortex about a stagnant core and turbulent flow thereafter. Vortex bursting causes a significant degradation in aerodynamic performance and is a limiting factor on aircraft maneuverability.

In symmetrical flow, the position of the breakdown depends on the angle of attack. At high incidence, both vortices burst symmetrically at about the same chord-wise station above the wing (Figure 3a). However, aircraft flying in their critical flight phases, i.e., takeoff, landing and, above all, maneuvering, often encounter asymmetrical vortex bursting even when their yaw angle is zero.

Asymmetrical vortex bursting is defined as the difference in burst location over the wing surface

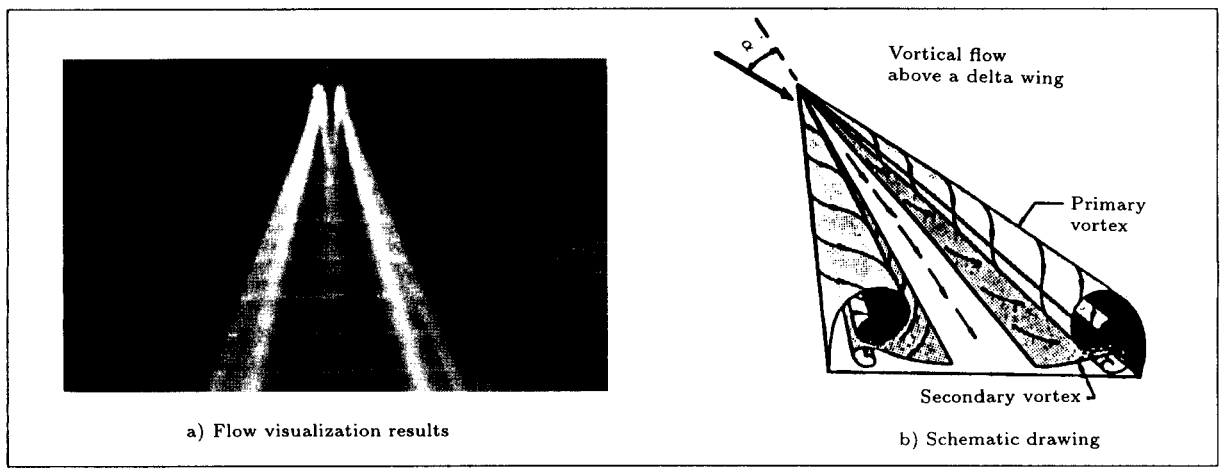

Figure 1. Top view of the vortices over a delta wing [1].

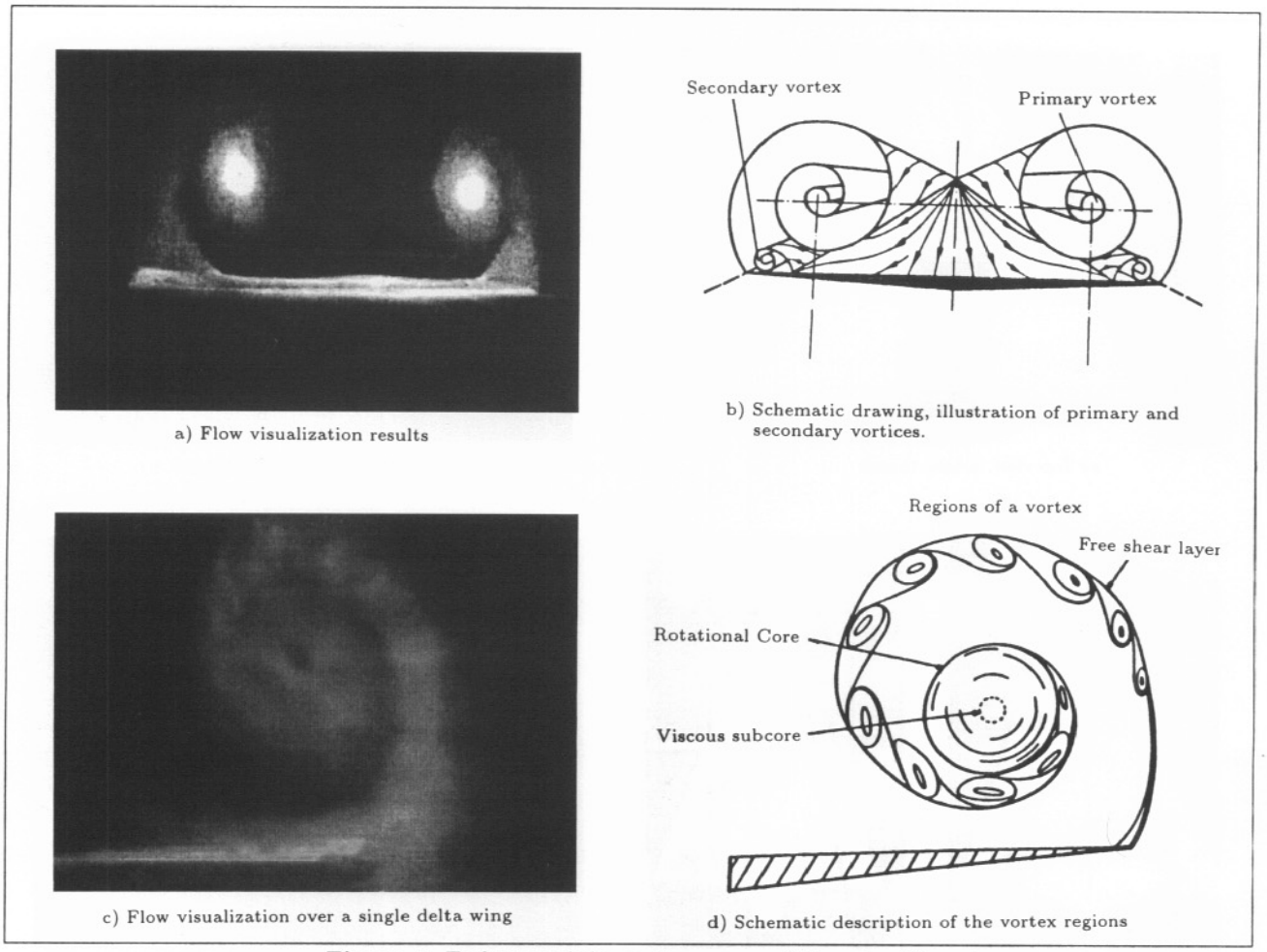

Figure 2. End view of the vortices over a delta wing [1].

between leeward and windward sides (Figure 4). This phenomenon appears to be a strong contributor to the highly nonlinear lateral-directional stability characteristics. These phenomena are observed at high angle of attack and limit the maneuvering performance of the aircraft, due to the loss of lateral stability. Control of asymmetrical bursting is, therefore, crucial when flying at very high angles of attack.

In a yawed situation, the effective sweep of the windward wing decreases while that of the leeward wing increases. As a result, the windward vortex core moves inboard and down close to the surface, with breakdown occurring much further forward than for the zero yaw case (Figure 4). In contrast, the leeward vortex core moves outboard and away from the surface, with the core breaking down far aft of the zero yaw case. The strength of the windward and leeward vortices increases and decreases, respectively, with an increasing yaw angle.

An unsteady nonlinear aerodynamic phenomenon experienced by highly swept delta wings at high angles of attack is known as wing rock. This motion is of particular interest to fighter aircraft equipped with highly swept wings useful for maneuvering, as well as supersonic transport that must operate at high angles of attack during the takeoff and landing phases [1].

The phenomenon is similar in many aspects to the limit cycle oscillation in pitch observed on blunt cylinder-flare bodies at high angles of attack, which is caused by asymmetric vortex shedding. Thus, the roll oscillation of a delta wing is self-excited and builds up to a limit cycle amplitude.

Wing rock creates a time-averaged loss in lift, which, in addition to the coupling of the longitudinal and lateral degrees of freedom, is another unwanted effect. Although there has been considerable research into the actual breakdown process, not much investigation appears to have been carried out to prevent this phenomenon and control the rocking that follows. Several theoretical models have been proposed to describe the motion and predict some of the aerodynamic derivatives [2].

The present investigation offers a new and simple analytical method for prediction of the amplitude and frequency of a slender wing undergoing rocking motion at high angles of attack, using the idea of an oscillating

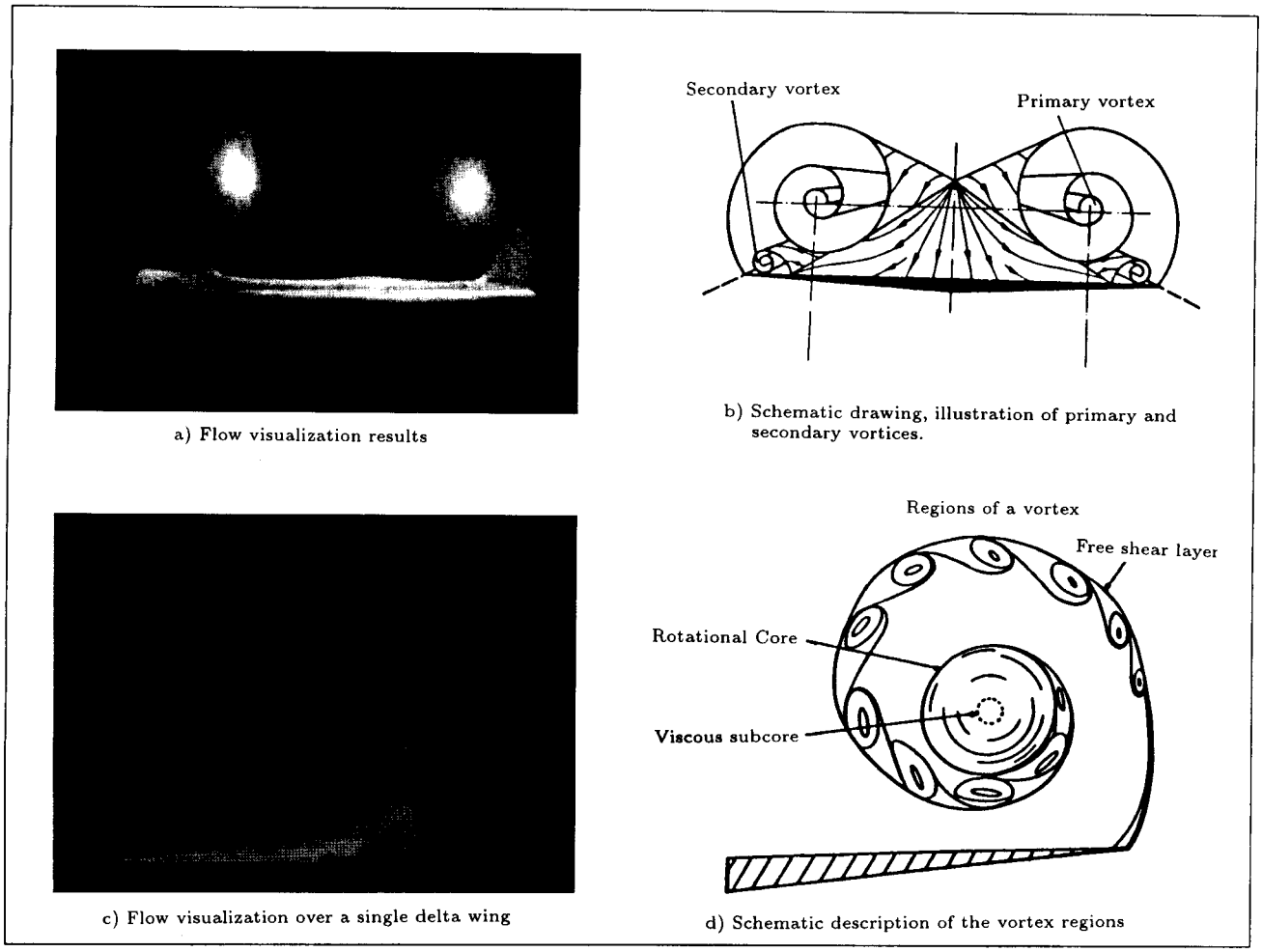

a) Flow visualization results

b) Schematic drawing, illustration of primary and secondary vortices.

c) Flow visualization over a single delta wing

d) Schematic description of the vortex regions

Figure 2. End view of the vortices over a delta wing [1].

between leeward and windward sides (Figure 4). This phenomenon appears to be a strong contributor to the highly nonlinear lateral-directional stability characteristics. These phenomena are observed at high angle of attack and limit the maneuvering performance of the aircraft, due to the loss of lateral stability. Control of asymmetrical bursting is, therefore, crucial when flying at very high angles of attack.

In a yawed situation, the effective sweep of the windward wing decreases while that of the leeward wing increases. As a result, the windward vortex core moves inboard and down close to the surface, with breakdown occurring much further forward than for the zero yaw case (Figure 4). In contrast, the leeward vortex core moves outboard and away from the surface, with the core breaking down far aft of the zero yaw case. The strength of the windward and leeward vortices increases and decreases, respectively, with an increasing yaw angle.

An unsteady nonlinear aerodynamic phenomenon experienced by highly swept delta wings at high angles of attack is known as wing rock. This motion is of particular interest to fighter aircraft equipped with highly swept wings useful for maneuvering, as well as supersonic transport that must operate at high angles of attack during the takeoff and landing phases [1].

The phenomenon is similar in many aspects to the limit cycle oscillation in pitch observed on blunt cylinder-flare bodies at high angles of attack, which is caused by asymmetric vortex shedding. Thus, the roll oscillation of a delta wing is self-excited and builds up to a limit cycle amplitude.

Wing rock creates a time-averaged loss in lift, which, in addition to the coupling of the longitudinal and lateral degrees of freedom, is another unwanted effect. Although there has been considerable research into the actual breakdown process, not much investigation appears to have been carried out to prevent this phenomenon and control the rocking that follows. Several theoretical models have been proposed to describe the motion and predict some of the aerodynamic derivatives [2].

The present investigation offers a new and simple analytical method for prediction of the amplitude and frequency of a slender wing undergoing rocking motion at high angles of attack, using the idea of an oscillating

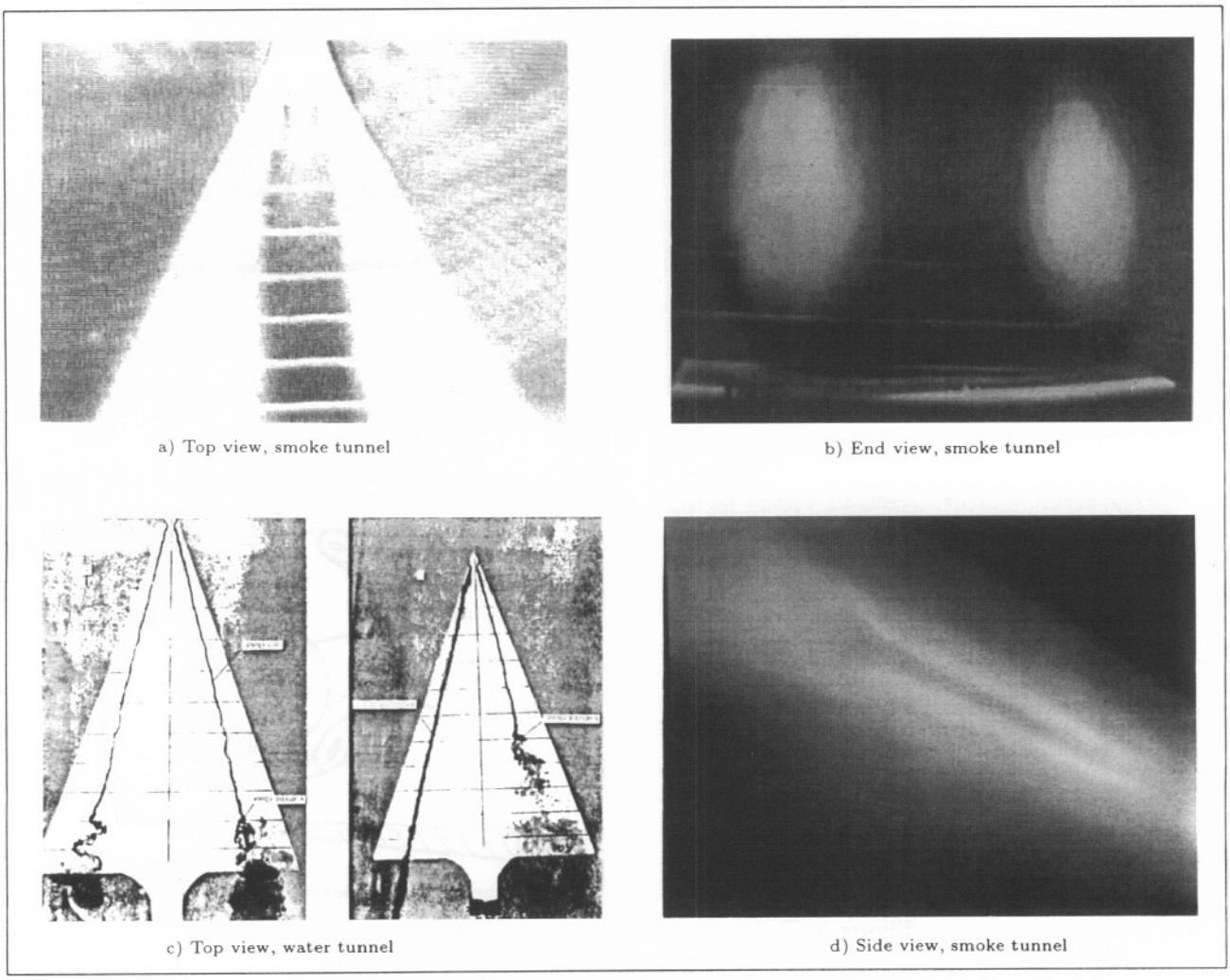

Figure 3. Illustration of the vortex bursting [1].

mass and spring. The method uses experimental data to calculate the aforementioned variables.

THEORETICAL DEVELOPMENTS

Several researchers [2-11] proposed different analytical methods for predicting the amplitude and frequency of delta wings undergoing rocking motion at nonzero side slip angles. These methods will not be reviewed in this paper. Interested readers are referred to [12] for details. The remainder of this paper focuses on the idea of an oscillating mass and spring to develop a method for predicting these variables for delta wings undergoing this motion at high angles of attack, when the side slip angle is zero. The idea is shown in Figure 5, where the vortices are simulated with two springs. As the angle of attack increases, the vortices become stronger. To simulate their strength, the springs are compressed, such that the compression force is equal to the change of lift produced by the vortices.

The potential lift that exists at small angles of attack could be simulated by locating springs at the center of the wing (not shown in Figure 5). However, as seen from Figure 3a, at high angles of attack, the entire flow over the wing is of a vortical type. When the wing rocks to one side, it causes the corresponding spring to compress until the resulting compression force overcomes the rocking force phenomenon, thus, changing the direction of the rocking motion.

With this idea, one can simulate the rocking motion with a free oscillation and calculate the corresponding natural frequency. The only question is that how much should the spring constants be to represent the corresponding potential and vortical lift? Also, the best place to locate the vortices must be known.

It has been shown that delta wing vortices are of a conical shape [13-15]. Using this result, looking from the top of the delta wing, the vortices look like a triangle, as shown in Figure 5. The flow visualization results of Figure 3a verify the validity of this hypothesis. Therefore, if C_b is the breakdown

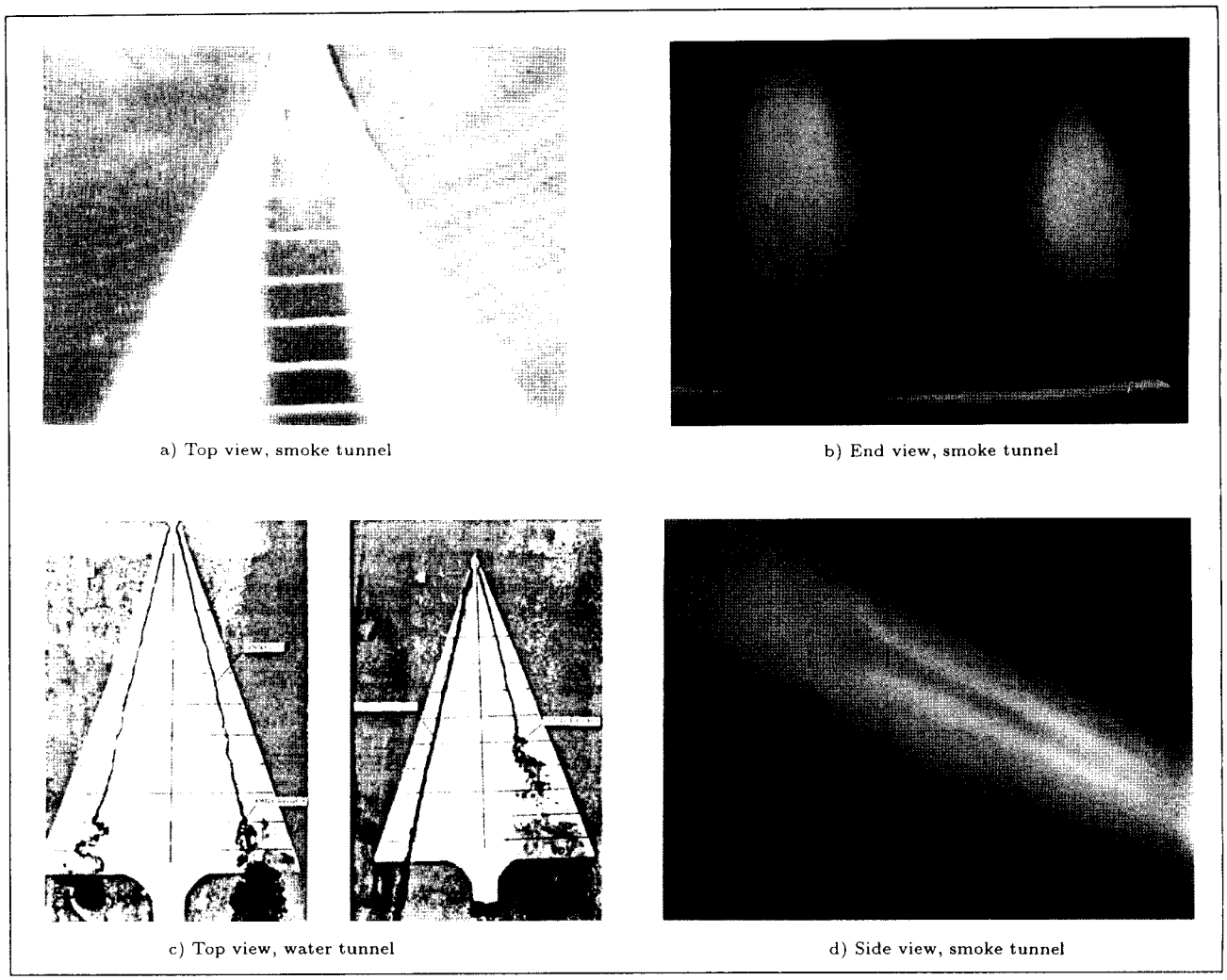

Figure 3. Illustration of the vortex bursting [1].

mass and spring. The method uses experimental data to calculate the aforementioned variables.

THEORETICAL DEVELOPMENTS

Several researchers [2-11] proposed different analytical methods for predicting the amplitude and frequency of delta wings undergoing rocking motion at nonzero side slip angles. These methods will not be reviewed in this paper. Interested readers are referred to [12] for details. The remainder of this paper focuses on the idea of an oscillating mass and spring to develop a method for predicting these variables for delta wings undergoing this motion at high angles of attack, when the side slip angle is zero. The idea is shown in Figure 5, where the vortices are simulated with two springs. As the angle of attack increases, the vortices become stronger. To simulate their strength, the springs are compressed, such that the compression force is equal to the change of lift produced by the vortices.

The potential lift that exists at small angles of attack could be simulated by locating springs at the center of the wing (not shown in Figure 5). However, as seen from Figure 3a, at high angles of attack, the entire flow over the wing is of a vortical type. When the wing rocks to one side, it causes the corresponding spring to compress until the resulting compression force overcomes the rocking force phenomenon, thus, changing the direction of the rocking motion.

With this idea, one can simulate the rocking motion with a free oscillation and calculate the corresponding natural frequency. The only question is that how much should the spring constants be to represent the corresponding potential and vortical lift? Also, the best place to locate the vortices must be known.

It has been shown that delta wing vortices are of a conical shape [13-15]. Using this result, looking from the top of the delta wing, the vortices look like a triangle, as shown in Figure 5. The flow visualization results of Figure 3a verify the validity of this hypothesis. Therefore, if C_b is the breakdown

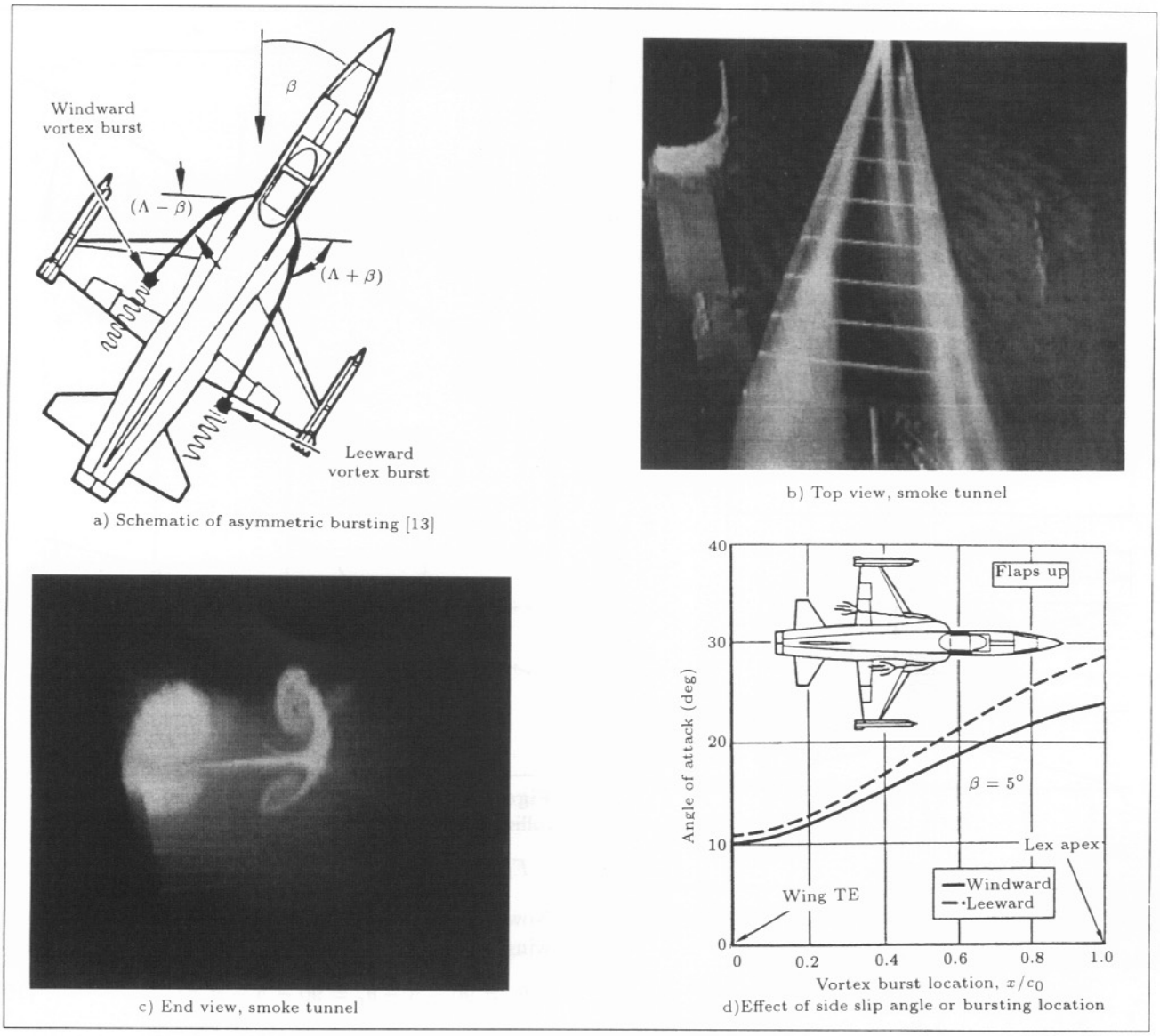

Figure 4. Asymmetrical vortex bursting [1].

distance and C_v the location of the corresponding force (equivalent spring force), then, one can write:

$$C_v = \frac{2}{3} n_1 C_b, \tag{1}$$

where n_1 is a constant that represents the amount of lift produced aft of the breakdown location. This is because bursting does not mean full flow separation over the surface (Figure 3a). It could be viewed as a dramatic structural change in the vortices. The potential lift comes from the pressure difference between the upper and lower surfaces. If C_p is the location of the corresponding potential lift over the wing surface then:

$$K_p C_p \sin\alpha = 2 n_2 K_v C_v \sin\alpha, \tag{2}$$

where K_p and K_v are the spring constants for potential and vortex lifts, respectively, and n_2 is the percent of potential lift available in the vortex force. It should be noted that the vortex force is the sum of the vortex and potential lift. From Figure 5:

$$\theta_p = n_3 \theta_v, \tag{3}$$

where n_3 is the ratio of two angles and is a constant. Now, let:

$$\frac{L_{p_u}}{L_{p_l}} = n_5. \tag{4}$$

Hence:

$$L_p = L_{p_u} + L_{p_l} = L_{p_l}(1 + n_5). \tag{5}$$

Since total lift is sum of the potential and vortex lifts, it is assumed that the potential lift is located at 2/3

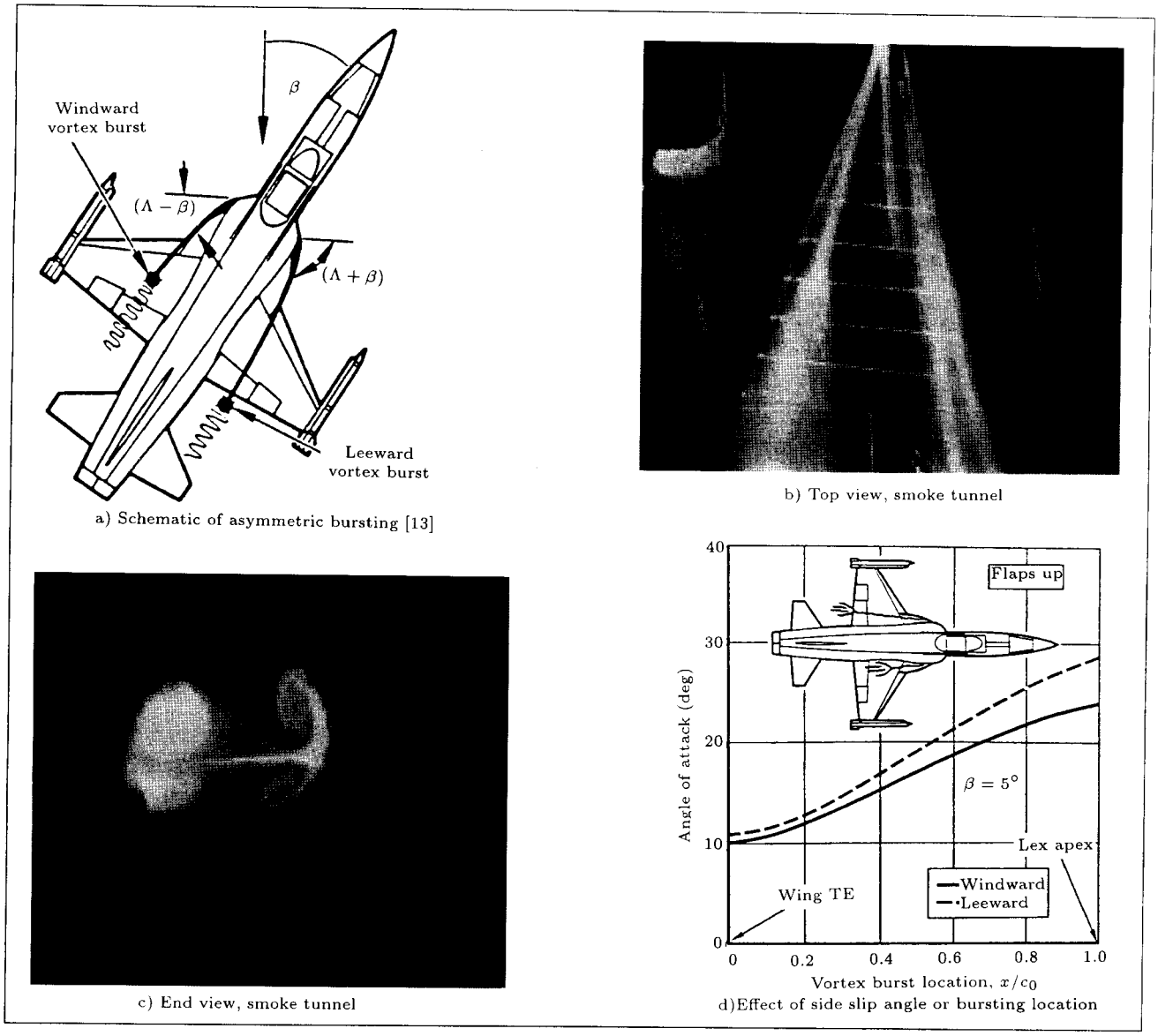

Figure 4. Asymmetrical vortex bursting [1].

distance and C_v the location of the corresponding force (equivalent spring force), then, one can write:

$$C_v = \frac{2}{3} n_1 C_b, \tag{1}$$

where n_1 is a constant that represents the amount of lift produced aft of the breakdown location. This is because bursting does not mean full flow separation over the surface (Figure 3a). It could be viewed as a dramatic structural change in the vortices. The potential lift comes from the pressure difference between the upper and lower surfaces. If C_p is the location of the corresponding potential lift over the wing surface then:

$$K_p C_p \sin\alpha = 2 n_2 K_v C_v \sin\alpha, \tag{2}$$

where K_p and K_v are the spring constants for potential and vortex lifts, respectively, and n_2 is the percent of potential lift available in the vortex force. It should be noted that the vortex force is the sum of the vortex and potential lift. From Figure 5:

$$\theta_p = n_3 \theta_v, \tag{3}$$

where n_3 is the ratio of two angles and is a constant. Now, let:

$$\frac{L_{p_u}}{L_{p_l}} = n_5. \tag{4}$$

Hence:

$$L_p = L_{p_u} + L_{p_l} = L_{p_l}(1 + n_5). \tag{5}$$

Since total lift is sum of the potential and vortex lifts, it is assumed that the potential lift is located at 2/3

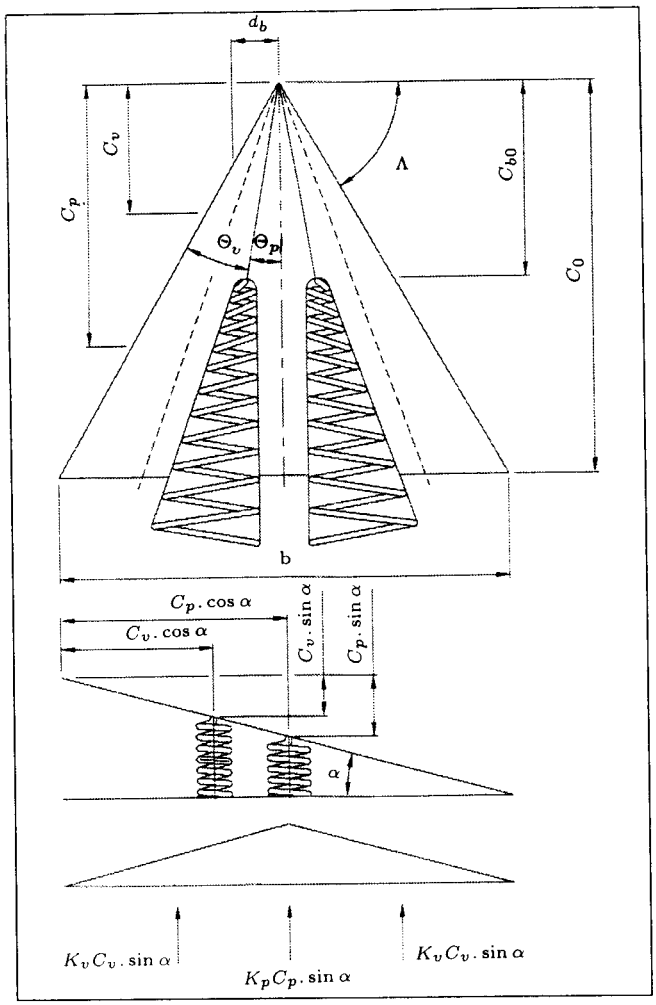

Figure 5. Simulation of vortex breakdown using springs.

$C_b n_4$, where n_4 varies between 0.0 and 1.0.

$$C_p = \frac{2}{3}\frac{L_{p_v}}{L_p}C_b n_4 + \frac{2}{3}\frac{L_{p_l}}{L_p}C_0. \tag{6}$$

After some algebra:

$$C_p = \frac{2}{3}\frac{n_4 n_5 C_b + C_0}{1+n_5}. \tag{7}$$

To calculate the spring constant, rotate the wing to a new angle of attack, α, and relocate the springs to a new position (see Figure 5). From this figure it can be seen that:

$$L = (2K_v C_v + K_p C_p)\sin\alpha = C_L \bar{q} S.$$

Consequently:

$$K_v = \frac{3C_L \bar{q} S}{4(n_1 C_b + n_1 n_2 C_b)\sin\alpha}. \tag{8}$$

CALCULATION OF THE NATURAL FREQUENCY ABOUT LONGITUDINAL AXIS (X AXIS)

From Figure 6, if F_1 is the vortical force created by the model at an angle of attack, α. Then:

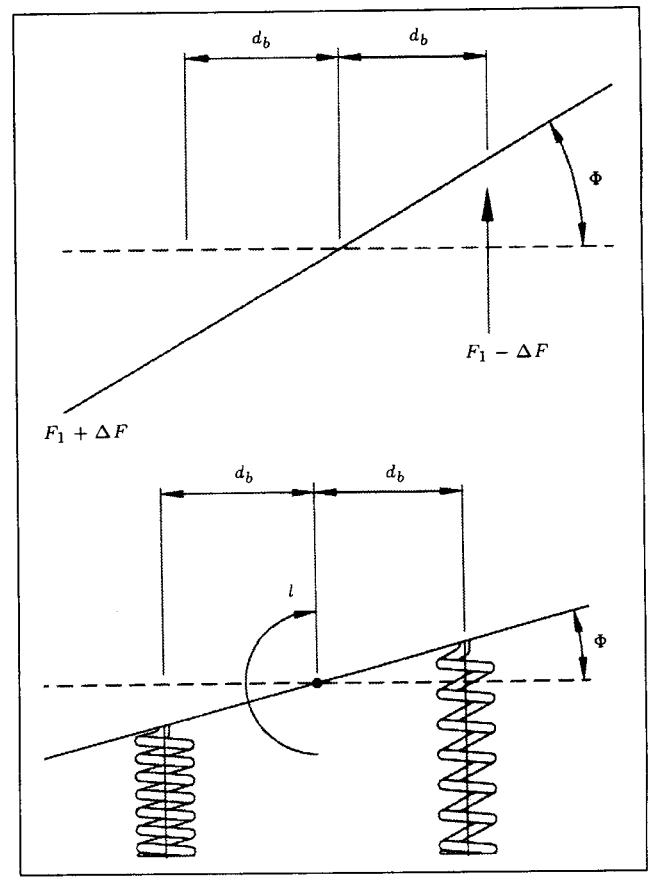

Figure 6. Creation of the natural frequency from the rolling moment.

$$F_1 = K_v C_v \sin\alpha. \tag{9}$$

Now, the distance from the applied vortical lift to the wing centerline, d_b, must be calculated. From Figure 5:

$$\theta_v = 90 - \Lambda - \theta_p = 90 - \Lambda - n_3\theta_v. \tag{10}$$

Hence:

$$\frac{d_b}{C_v} = \tan(\theta_p + \frac{\theta_v}{2}).$$

So:

$$d_b = \frac{2}{3}n_1 C_b \tan(\theta_p + \frac{\theta_v}{2}). \tag{11}$$

Now, the equation for the natural frequency of the wing oscillating about X axis becomes:

$$(F_1 + K_v\phi d_b)d_b\cos\alpha - (F_1 - K_v\phi d_b\cos\alpha) = -I_{xx}\ddot{\phi}, \tag{12}$$

where the dot symbol denotes differentiation, with respect to time, i.e. $\dot{\phi} = \frac{\partial\phi}{\partial t}$ and $\ddot{\phi} = \frac{\partial^2\phi}{\partial t^2}$.

Now, to get the normal force, multiply the spring forces by $\cos\alpha$. Then:

$$2K_v\phi d_b^2\cos\alpha = -I_{xx}\ddot{\phi}. \tag{13}$$

Substituting for d_b from Equation 11, Equation 13 becomes:

$$\ddot{\phi} + \left(\frac{8}{9}\frac{K_v}{I_{xx}} C_b^2 n_1^2 \tan^2\left(\theta_p + \frac{\theta_v}{2}\right)\cos\alpha\right)\phi = 0. \tag{14}$$

Now, define:

$$\omega_x^2 = \frac{8}{9I_{xx}} K_v n_1^2 C_b^2 \tan^2(n_3 + \frac{1}{2})\theta_v \cos\alpha. \tag{15}$$

So Equation 14 becomes:

$$\ddot{\phi} + \omega_x^2 \phi = 0. \tag{16}$$

Equation 16 is a simple second order differential equation. It has a famous analytical solution as follows:

$$\phi = C_1 \cos\omega_x t + C_2 \sin\omega_x t. \tag{17}$$

Subjected to the following boundary condition: at $t = 0, \varphi = 0$, hence, $C_1 = 0$. Thus:

$$\phi = C_2 \sin\omega_x t. \tag{18}$$

On the other hand, $C_2 = \varphi_{\max} = \varphi_m$ and Equation 17 becomes:

$$\phi = \phi_m \sin\omega_x t. \tag{19}$$

Note that the created rolling moment can only rotate the wing by an amount equal to φ_m. From Figure 6, one can write:

$$[(F_1 + K_v d_b \sin\phi) d_b \cos\phi]\cos\alpha$$
$$- [(F_1 - K_v d_b \sin\phi) d_b \cos\phi]\cos\alpha = -C_l \bar{q} S b. \tag{20}$$

Simplify, to get:

$$\sin 2\phi = -\frac{C_l \bar{q} S b}{K_v d_b^2 \cos\alpha}. \tag{21}$$

Now, using Equations 8 and 11, the above equation reduces to:

$$\frac{\tan^2(n_3 + \frac{1}{2})\theta_v}{n_2 + 1} = -\frac{3C_l b}{n_1 C_b C_L \sin 2\phi}\tan\alpha. \tag{22}$$

Substitute the above result into Equation 15 to get:

$$\omega_x^2 = -\frac{2C_l \bar{q} S b}{I_{xx}} \frac{1}{\sin 2\phi}. \tag{23}$$

From Figures 7 and 8 taken from [8] and [16], respectively, it is obvious that $|C_{l_{\max}}|$ occurs at $|\varphi_{max}|$ thus:

$$\omega_x^2 = -\frac{2C_{l_{\max}} \bar{q} S b}{I_{xx}} \frac{1}{\sin 2\phi_{\max}}.$$

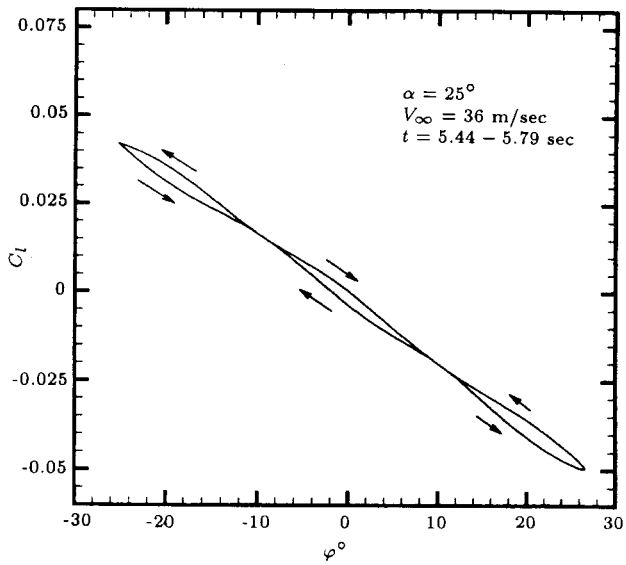

Figure 7. Variation of the rolling moment with ϕ [16].

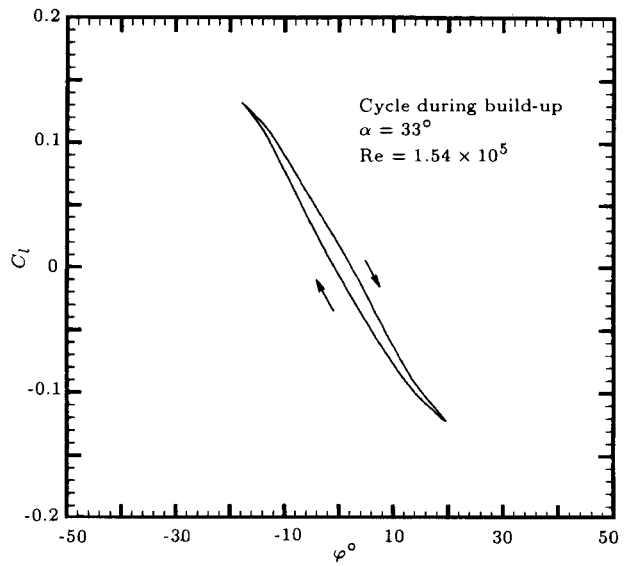

Figure 8. Variation of the rolling moment with ϕ [16].

Figure 7 is constructed from the seventeenth cycles of the roll angle variation of the wing, used in [8]. Experimental variation of the roll angle versus time for this wing is also shown in Figure 9. The rolling moment loop shown in Figure 7 is calculated using the experimental data of Figure 9. Also, from Figures 7 and 8 one can assume that C_l varies linearly with φ. Hence, the hysteresis loop in C_l variation can be neglected. Therefore, one can write:

$$C_l = C_{l_\phi}\phi, \tag{24}$$

or:

$$C_{l\max} = C_{l_\phi}\phi_{\max}, \tag{25}$$

and:

$$\omega_x^2 \approx -\frac{\bar{q} S b}{I_{xx}} C_{l_\phi}. \tag{26}$$

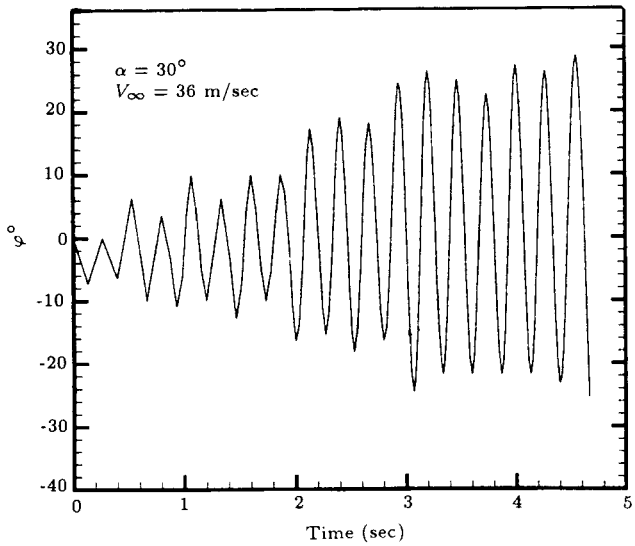

Figure 9. Time variation of rolling moment [16].

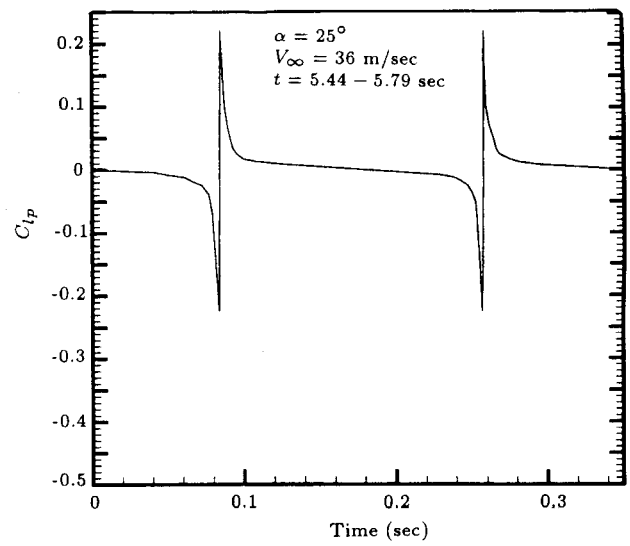

Figure 10. Variation of C_{l_p} with time.

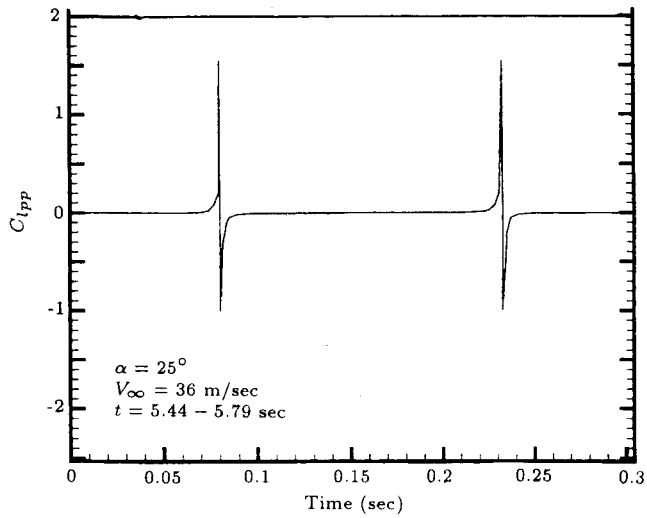

Figure 11. Variation of $C_{l_{p_p}}$ with time.

Applying the above equation to the wing of [16], one can easily calculate frequency and period of oscillation. Substituting the constants into Equation 26, one obtains:

$$\omega_x = 18.5 \text{ rad/sec},$$

$$f = 2.946 \text{ HZ},$$

$$\tau = \frac{1}{f} = 0.34 \text{ sec}.$$

Comparing the results of this simple theory with the experimental data of [10], one obtains $\Delta\tau = \tau_{\text{theoretical}} - \tau_{\text{experimental}} = 0.01$ sec. This difference is an indication of the error involved in the present simple theory using the spring and mass concept. From the former equations, one can calculate C_{l_p} and $C_{l_{p_p}}$. The results are:

$$C_{l_p} = -\frac{I_{xx}\omega_x}{qS}\frac{\omega_x \phi}{p}, \tag{27}$$

$$C_{l_{p_p}} = \frac{I_{xx}}{\phi_m \bar{q} S b}\frac{\tan \omega_x t}{\cos \omega_x t}. \tag{28}$$

Figures 10 and 11 show the variations of C_{l_p} and $C_{l_{p_p}}$ with time for the wing of [8]. Thus, one can conclude that the rocking motion of a delta wing along it's longitudinal axis can be approximated as a sinusoidal motion and the corresponding aerodynamic forces can be simulated by three springs representing the potential and vortical forces. When the wing falls into the rocking motion, it will also oscillate about the Z axis. Using the same procedure, ω_z can be predicted too.

The following will show the procedure for calculating the natural frequency along the Z axis. If Equation 12 is multiplied by $\sin\alpha$ to get the horizontal force, after some algebra, the following equation will be obtained:

$$\ddot{\Psi} + \left[\frac{8}{9}\frac{K_v}{I_{zz}} n_1^2 C_b^2 \tan^2(n_3 + \frac{1}{2})\theta_v \sin\alpha\right]\Psi = 0. \tag{29}$$

Define:

$$\omega_z^2 = \left[\frac{8}{9}\frac{K_v}{I_{zz}} n_1^2 C_b^2 \tan^2(n_3 + \frac{1}{2}) \sin\alpha\right]\theta_v. \tag{30}$$

Dividing Equation 15 by Equation 30 to get:

$$\frac{\omega_x^2}{\omega_z^2} = \frac{I_{zz}}{I_{xx}}\frac{1}{\tan\alpha}, \tag{31}$$

or:

$$\omega_z^2 = -\frac{2C_n \bar{q} S b}{I_{zz} \sin 2\Psi}, \tag{32}$$

and:

$$\frac{C_l}{C_n} = \frac{\sin 2\phi}{\sin 2\Psi} \frac{1}{\tan \alpha}. \tag{33}$$

For small angles, Equation 33 reduces to:

$$\frac{C_l}{C_n} = \frac{\phi}{\Psi} \frac{1}{\tan \alpha}, \tag{34}$$

or:

$$\frac{C_{l\max}}{C_{n\max}} = \frac{\phi_{\max}}{\Psi_{\max}} \frac{1}{\tan \alpha}. \tag{35}$$

However, it should be noted that as the ratio of $\frac{I_{zz}}{I_{xx}}$ becomes smaller, the accuracy of the presented single degree of freedom dynamic model increases and vice-versa. If this ratio for a body is a large number, one must use three degrees of freedom models.

CALCULATION OF THE OSCILLATION AMPLITUDE

As mentioned before, at high angles of attack, vortices over the wing surface burst, degrading the aerodynamic forces and moments. At the zero angle of roll, i.e. $\phi = 0$, the burst position over the left and right sides of the wing surface is symmetric but when $\phi \neq 0$, asymmetrical bursting occurs, a phenomenon that causes roll oscillation shown in Figure 12. From this figure, using the idea of spring and mass constants and relating the lift of the wing at various angles of attack to the area covered by the springs as previously shown, one can write:

$$L_{N_R} = \frac{1}{2} C_N \bar{q} C_{b_R}^2 \left[\tan(\theta_p + \theta_v) - \tan\theta_p\right], \tag{36}$$

$$L_{N_L} = \frac{1}{2} C_N \bar{q} C_{b_L}^2 \left[\tan(\theta_p + \theta_v) - \tan\theta_p\right]. \tag{37}$$

The distances from the point of application of these forces to the wing center line are l_L and l_R respectively, then, from Figure 9.

$$l_L - l_R = \left(\frac{C_{b_L}^3}{C_{b_R}^3} - 1\right) l_R = C_l \bar{q} S b. \tag{38}$$

But:

$$1_R = \frac{1}{2} C_N \bar{q} C_{b_R}^2 [\tan(\theta_p + \theta_v) - \tan\theta_p]$$

$$\frac{2}{3} C_{b_R} \tan(\theta_p + \frac{\theta_v}{2}), \tag{39}$$

substitute for l_R into Equation 38 to get:

$$C_l = \frac{C_N}{3Sb}\left[\tan(\theta_p + \frac{\theta_v}{2})(\tan(\theta_p + \theta_v) - \tan\theta_p)\right](C_{b_L}^3 - C_{b_R}^3), \tag{40}$$

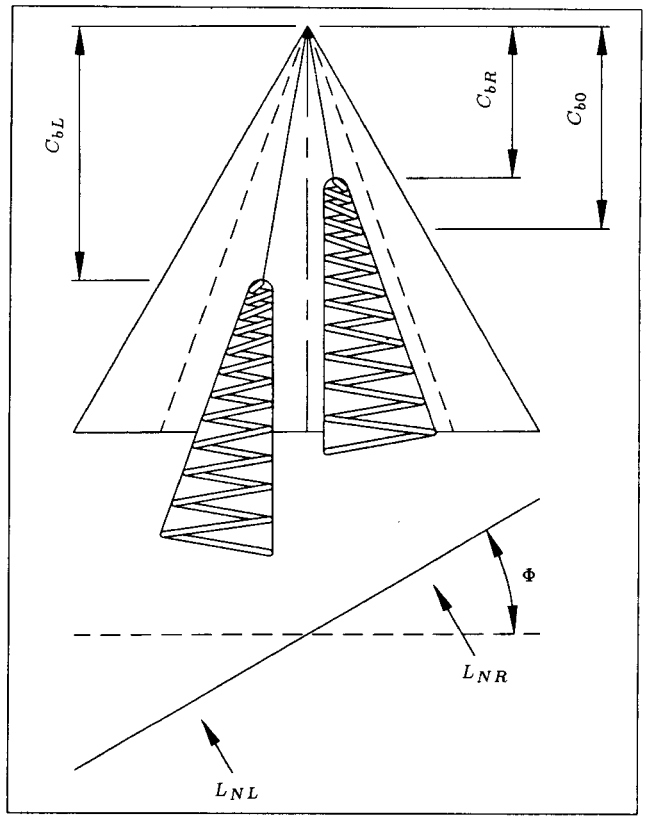

Figure 12. Asymmetrical vortex burst simulation.

or:

$$C_l = \frac{C_N C_0^3}{3Sb}\left[\tan(\theta_p + \frac{\theta_v}{2})(\tan(\theta_p + \theta_v) - \tan\theta_p)\right](X_L^3 - X_R^3). \tag{41}$$

Assuming $X_{R_\phi} = -X_{L_\phi}$ then:

$$C_{l_\phi} = \frac{C_N C_0^3}{3Sb}\left[\tan(\theta_p + \frac{\theta_v}{2})(\tan(\theta_p + \theta_v) - \tan\theta_p)\right](X_L^2 + X_R^2)X_\phi, \tag{42}$$

where:

$$X_\phi = \frac{dX}{d\phi}, \tag{43}$$

and:

$$X_L = x_0 + X, \quad X_R = x_0 - X.$$

Then:

$$\frac{C_l}{C_{l_\phi}} = \frac{1}{3}\frac{X_L^3 - X_R^3}{X_L^2 + X_R^2} X_\phi, \tag{44}$$

x_0 is the initial location of the symmetric burst point over the wing and is independent of time. X is the percent of the wing covered by the burst vortices and,

of course, is time dependent. Now, since $C_l = C_{l_\phi}\phi$, then:

$$\phi = \frac{1}{3}\frac{X_L^3 - X_R^3}{X_L^2 + X_R^2} X_\phi. \tag{45}$$

Substitute for X_φ, X_L and X_R into Equation 45 to get:

$$3\phi d\phi = \frac{3x_0 X + X^3}{x_0^2 + X^2} dX. \tag{46}$$

Integrate the above equation from $\varphi = 0$ to $\varphi = \varphi_m$ for $X = 0$ to $X = X_m$ the following is obtained:

$$\phi_m^2 = \frac{1}{3}X_m^2 + \frac{2}{3}x_0^2 \ln\left[\frac{x_0^2 + X_m^2}{x_0^2}\right]. \tag{47}$$

Note that X is a function of time and could be written as $X = X_m \sin(\omega t)$. Then:

$$\begin{aligned}\phi &= \left(\phi_m \sin(\omega_x t)\right)^2 \\ &= \left[\frac{1}{3}\left(e^{-\frac{z}{12}} X_m \sin(\omega_b t)\right)^2 \right. \\ &\quad \left. + \frac{2}{3}x_0^2 \ln\left(\frac{x_0^2 + \left(e^{-\frac{z}{12}} X_m \sin(\omega_b t)\right)^2}{x_0^2}\right)\right]^{\frac{1}{2}},\end{aligned} \tag{48}$$

where z depends on several parameters such as α, Λ, Re, i.e. $z = f(\alpha, \Lambda, Re) = \text{const}$.

Equation 47 is the main result of the present investigation. However, various parameters are still needed that must be obtained experimentally or theoretically before solving ϕ from Equations 47 or 48.

Table 1 compares the predicted values of φ from Equation 47 with those obtained from experimental results of [8,16] at various angles of attack. For all angles of attack tested, the results are in good agreement, which indicates the accuracy of this simple method. Equation 47 is the first equation that relates the oscillation amplitude to the breakdown location over the wing surface, a phenomenon that occurs at high angles of attack. From the above comparison, it could be concluded that the aerodynamic force of the vortices over the wing surface (lift force) is directly related to the wing area covered by these vortices. It should be noted that the present paper calculates only $\varphi_{\max}$, not φ.

Table 1. Comparison between present method and experiments.

α°	$\bar{x}_0$	$\overline{X}_m$	$\phi^\circ_{\max}$ (Experiment)	$\phi^\circ_{\max}$ (Present Method)
22*	1.0	0.5	27.2	27.6
25*	1.0	0.33	29.3	29.2
32*	1.0	0.32	22.0	21.3
40**	0.75	0.43	24	23.5
45**	0.45	0.24	12.8	13.2
50**	0.34	0.16	8.5	8.9

*: Experimental data from [8]

**: Experimental data from [11]

CONCLUSION

A simple method has been developed that is capable of predicting the amplitude and frequency of oscillation of highly swept delta wings undergoing rocking motion at high angles of attack. The results are in excellent agreement with those obtained by experimental studies for wings with sweep angles of 76 and 80 degrees. However the methodology needs a few variables that should be obtained experimentally or theoretically. Presently these variables are obtained experimentally.

Both amplitude and oscillation frequency depend on the wing sweep angle, wing angle of attack and Reynolds number. Wing thickness does not seem to have a significant effect on the rocking motion. Further studies into the wing rocking motion are needed to relate the flow field properties, such as vortex breakdown, vortex position and some other parameters, to the dynamic rolling moments. In the meantime, the described simple model, along with some experimental data, presents a rapid tool for prediction of the maximum possible wing rock amplitude and frequency.

NOMENCLATURE

K_p	spring constant for potential lift
K_v	constant for vortex lift
α	angle of attack
Ψ	heading angle
Λ	wing sweep angle
φ	roll angle
C_l	rolling moment coefficient
C_n	yawing moment coefficient
C_L	lift coefficient
C_N	normal force coefficient
$\bar{q}$	dynamic pressure
S	wing area
b	wing span
l_B	rolling moment
L_{p_u}	potential lift for the upper surface
L_{p_l}	potential lift for the lower surface
I_{xx}	moment of inertia about X axis
I_{zz}	moment of inertia about Z axis
C_0	wing chord

C_b breakdown distance from the wing apex

C_v location of the vortical lift force over the wing

C_p location of the potential lift

REFERENCES

1. Soltani, M.R. "An experimental study of the relationship between forces and moments and vortex breakdown on a pitching delta wing", Ph.D. Thesis, University of Illinois at Urbana-Champaign (Dec. 1992).
2. Lan, C.E. "Theoretical prediction of wing rocking", AGARD-CP-38, pp 32-1 to 32-13 (1985).
3. Narayan, K.R. "Types of flow on the lee side of delta wings", *Prog. Aerospace Sci.*, **33**, pp 167-257 (1997).
4. Ericsson, L.E. "Effect of angle of attack on roll characteristics of 65 degree delta wing", *Journal of Aircraft*, **34**(4), pp 573-575 (1997).
5. Kandil, O.A. "Three dimensional simulation of slender delta wing rock and divergence", *AIAA Journal*, pp 1-11 (1992).
6. Lang, J.D. "Unsteady aerodynamics and dynamics of aircraft maneuverability", AGARD-CP-386, pp 29-1 to 29-18 (1985).
7. Ericsson, L.E. "Analytic prediction of maximum amplitude of slender wing rock", *Journal of Aircraft*, **26**(1), pp 35-39 (1989).
8. Levin, D. "Dynamic load measurements with delta wings undergoing self induced roll oscillations", *Journal of Aircraft*, **21**(1), pp 30-36 (1984).
9. Ericsson, L.E. "The fluid mechanics of slender wing rock", *Journal of Aircraft*, **21**(5) (1984).
10. Walton, J. and Katz, J. "Reduction of wing rock amplitudes using leading-edge vortex manipulations", AIAA, Reno, NV, pp 92-0279 (Jan. 6-9 1992).
11. Arena, Jr. A.S. and Nelson, R.C. "The effect of asymmetric vortex wake characteristics on a slender delta wing undergoing wing rock motion", AIAA-89-3348 (1989).
12. Ebrahimi, S.A. "The prediction of amplitude and frequency of wing rock for delta wings", Master Thesis, Sharif University of Technology (1998).
13. Kjelgard, S.O. "The flow field over a 75 degree swept delta wing at 20.5 degrees angle of attack", AIAA-86-1775 (1986).
14. Hoejamakers, H.W. et al. "Vortex flow over delta and double delta wings", *Journal of Aircraft*, **20**(9) (1983).
15. Beecham, L.J. and Titchener, I.M. "Some notes on an approximate solution for the free oscillation characteristics of non-linear systems typified by $\ddot{X} + F(X) = 0$", British Aeronautical Research Council, R & M No. 3651 (1989).
16. Moris, S.L. and Ward, D.T. "A video-based experimental investigation of wing rock", AIAA-89-3349 (1989).